THE JOURNAL OF BIOLOGICAL CHEMISTRY VOL. 287, NO. 27, pp. 22509–22520, June 29, 2012

Expression of *Saccharomyces cerevisiae* Sdh3p and Sdh4p Paralogs Results in Catalytically Active Succinate Dehydrogenase Isoenzymes*[S]

Received for publication, January 23, 2012, and in revised form, April 20, 2012 Published, JBC Papers in Press, May 9, 2012, DOI 10.1074/jbc.M112.344275

Samuel S. W. Szeto (司徒尚閎)[1], Stacey N. Reinke, Kayode S. Oyedotun, Brian D. Sykes, and Bernard D. Lemire[2]
From the Department of Biochemistry, University of Alberta, Edmonton, Alberta T6G 2H7, Canada

Background: Succinate dehydrogenase is a tetrameric, mitochondrial membrane protein needed for respiratory energy generation.
Results: Yeast succinate dehydrogenase containing Sdh3p and Sdh4p paralogs is catalytically active.
Conclusion: Expression of paralogous subunits results in enzymes with novel kinetic properties.
Significance: At least four functional succinate dehydrogenase isoenzymes containing zero, one, or two paralogs can be expressed in yeast mitochondria.

Succinate dehydrogenase (SDH), also known as complex II, is required for respiratory growth; it couples the oxidation of succinate to the reduction of ubiquinone. The enzyme is composed of two domains. A membrane-extrinsic catalytic domain composed of the Sdh1p and Sdh2p subunits harbors the flavin and iron-sulfur cluster cofactors. A membrane-intrinsic domain composed of the Sdh3p and Sdh4p subunits interacts with ubiquinone and may coordinate a b-type heme. In many organisms, including *Saccharomyces cerevisiae*, possible alternative SDH subunits have been identified in the genome. *S. cerevisiae* contains one paralog of the Sdh3p subunit, Shh3p (YMR118c), and two paralogs of the Sdh4p subunit, Shh4p (YLR164w) and Tim18p (YOR297c). We cloned and expressed these alternative subunits. Shh3p and Shh4p were able to complement Δ*sdh3* and Δ*sdh4* deletion mutants, respectively, and support respiratory growth. Tim18p was unable to do so. Microarray and proteomics data indicate that the paralogs are expressed under respiratory and other more restrictive growth conditions. Strains expressing hybrid SDH enzymes have distinct metabolic profiles that we distinguished by ^{1}H NMR analysis of metabolites. Surprisingly, the Sdh3p subunit can form SDH isoenzymes with Sdh4p or with Shh4p as well as be a subunit of the TIM22 mitochondrial protein import complex.

Respiratory growth in the yeast *Saccharomyces cerevisiae* requires functional succinate dehydrogenase (SDH),[3] a respiratory chain enzyme localized to the mitochondrial inner membrane (1). SDH is also known as succinate:ubiquinone oxidoreductase or complex II. It couples the oxidation of succinate to fumarate in the Krebs cycle with the reduction of ubiquinone to ubiquinol. SDH comprises two domains: a catalytic, membrane-extrinsic domain containing the Sdh1p and Sdh2p subunits and a membrane domain containing the Sdh3p and Sdh4p subunits. The Sdh1p subunit contains the active site where succinate binds near a covalently attached flavin adenine dinucleotide (FAD). The three iron-sulfur clusters located in Sdh2p form a pathway for electrons derived from succinate to travel to the proximal quinone-binding site residing in the Sdh3p and Sdh4p subunits. The presence of both a b-type heme and a second, distal quinone-binding site in the membrane domain remain controversial.

In recent years, there has been considerable interest in the human SDH, which is also composed of four subunits referred to as SDHA to SDHD (2–6). Most mutations of SDHA result in Leigh syndrome, a severe, progressive neurodegenerative disease (2), but recently, SDHA was identified as a new paraganglioma and pheochromocytoma susceptibility gene (7). In contrast, mutations in SDHB, SDHC, or SDHD do not result in Leigh syndrome but rather in cancers such as pheochromocytomas (catechol-secreting tumors usually found in the adrenal medulla), paragangliomas (benign, vascularized tumors in the head and neck), renal cell carcinoma, gastrointestinal stromal tumors, and neuroblastoma (2, 8, 9). In addition, the SDHC and SDHD subunits may also regulate apoptosis (10–12).

The succinate:quinone oxidoreductase family to which SDH belongs is structurally diverse and can be divided into five classes based on membrane domain subunit composition and heme content (13). Fumarate reductases, also members of this family, are anaerobically expressed enzymes that oxidize quinols and reduce fumarate to succinate, the reverse of the SDH reaction (14). The Sdh1p/Sdh2p catalytic dimer is believed to have evolved from the association of a soluble fumarate reductase containing non-covalent FAD (in the Sdh1p subunit) with a ferredoxin electron donor (in the Sdh2p subunit) (15). For type C enzymes like the SDH of eukaryotic mitochondria, the

* This work was supported by Canadian Institutes of Health Research Grants MT-15290 and MOP-84455 (to B. D. L.) and MOP-37769 (to B. D. S.).
[S] This article contains supplemental Tables I–IV and Figs. 1–3.
[1] Present address: Inst. of Medical Biology, *Agency for Science, Technology and Research* (A*STAR), Singapore.
[2] To whom correspondence should be addressed: Dept. of Biochemistry, School of Translational Medicine, University of Alberta, Edmonton, Alberta T6G 2H7, Canada. Tel.: 780-492-4853; Fax: 780-492-0886; E-mail: bernard.lemire@ualberta.ca.
[3] The abbreviations used are: SDH, succinate dehydrogenase; DB, decylubiquinone; DCPIP, dichlorophenol indophenol; PLS-DA, partial least square discriminate analysis; ts, temperature-sensitive; DSS-d_6, 2,2-dimethyl-2-sila-3,3,4,4,5,5-hexadeuteropentane sulfonic acid; CV-ANOVA, analysis of variance testing of cross-validated predictive residuals; PMS, phenazine methosulfate.

catalytic dimer became membrane-bound by associating with a pair of membrane proteins coordinating two hemes (13). Attachment to the membrane presumably provided a bioenergetic advantage. Later, the FAD became covalently attached, favoring succinate oxidation over fumarate reduction. Sites for quinol chemistry were optimized, and one of the hemes was lost. Prokaryotes and eukaryotes now express a number of fumarate reductase and SDH variants containing zero, one, or two hemes with membrane domains of different architectures optimized to utilize a variety of quinone species. Some genomes, such as that of *Escherichia coli*, contain genes for separate fumarate reductase and SDH enzymes.

The complexity of succinate:quinone oxidoreductases can be exploited to provide developmental advantages. The presence of more than one SDH subunit isoform can confer alternative enzymatic properties on the enzyme. For example, the parasitic nematode *Ascaris suum* complex II changes subunit composition during its life cycle (16). The adult and third stage larval forms of this intestinal parasite contain different subunits equivalent to Sdh1p and Sdh4p, whereas the subunits equivalent to Sdh2p and Sdh3p subunits remain the same. The larval enzyme acts preferentially as a fumarate reductase, whereas the adult enzyme is optimized for succinate oxidation. In the parasitic sheep nematode *Haemonchus contortus*, differential expression of Sdh2p subunit isoforms occurs when the SDH of free living third stage larvae that is poised for succinate oxidation is converted to an enzyme that favors fumarate reduction in the adult stage (17). In the case of *Arabidopsis thaliana*, three genes for Sdh2p subunits are present; one of these, *SDH2–3* is only expressed in embryonic and not vegetative tissues (18).

The *S. cerevisiae* genome also contains SDH subunit isoforms. An alternative isoform of Sdh1p (YJL045w) referred to as Sdh1bp was identified; it has 84% sequence identity with Sdh1p and is able to complement a Δ*sdh1* strain when expressed from a multicopy plasmid (19). An Sdh3p homolog called YMR118c is a mitochondrial membrane protein of 196 amino acid residues with 57% sequence identity and 72% similarity to Sdh3p. Two Sdh4p homologs, YLR164w and YOR297c, are respectively 52 and 36% identical and 74 and 57% similar to Sdh4p. YOR297c is also called Tim18p, a subunit of the TIM22 mitochondrial inner membrane import complex, which mediates the import of polytopic inner membrane proteins lacking cleavable presequences (20, 21). *TIM18* was identified as a suppressor of the temperature-sensitive (ts) *tim54-1* mutant. Tim18p can be co-immunoprecipitated with Tim54p, Tim22p, and Tim12p. Furthermore, disruption of the *TIM18* gene is synthetic lethal with *tim54*(*ts*), *tim9*(*ts*), and *tim10*(*ts*) mutations, confirming that Tim18p is an authentic component of the import machinery (20, 21). Conversely, *SDH4* or *YLR164w* do not suppress a *tim54*(*ts*) mutation, and Sdh4p and YLR164w are not found in association with Tim18p. Tim18p, like Sdh4p, contains three transmembrane helices with its amino terminus in the matrix (20, 21). Despite the high sequence identity between Sdh4p and Tim18p, current evidence suggests they are functionally independent.

More recently, Sdh3p was also found in a subcomplex with Tim18p as part of the TIM22 inner membrane translocase complex (22). Sdh4p did not have a role in the TIM22 complex. Overexpression of Sdh3p partially suppressed the growth defect of a *tim22-44* mutant, demonstrating a functional role in the translocase (22).

In this study, we investigated the ability of YMR118c to substitute for Sdh3p and for YLR164w and YOR297c/Tim18p to substitute for Sdh4p. We found that YMR118c and YLR164w, which have been given the gene names *SHH3* (Sdh3 homolog) and *SHH4* (Sdh4 homolog) (22), respectively, were able to complement Δ*sdh3* and Δ*sdh4* strains and create respiration-competent SDH isoenzymes. In contrast, YOR297c/Tim18p was not able to complement a Δ*sdh4* deletion strain even when overexpressed. We characterized the kinetic properties of hybrid SDH enzymes containing one or both of these paralogs. Using ^{1}H NMR, we also show that expression of one or both complementing paralogs resulted in distinct metabotypes. Sdh3p is capable of forming at least three different protein complexes in the mitochondrial inner membrane and plays important roles in energy generation and mitochondrial biogenesis.

EXPERIMENTAL PROCEDURES

Strains, Media, and Culture Conditions—The *S. cerevisiae* strains sdh3W1 (MH125, *sdh3*::*TRP1*), sdh4W2 (MH125, *sdh4*::*TRP1*), and sdh3W1/4K6 (YPH499, *sdh3*::*TRP1*, *sdh4*::*LYS2*) and the *Escherichia coli* strain DH5α have been described previously (23). The yeast media used have been described (24). All cultures grown under non-selective conditions were monitored for plasmid loss.

Cloning of SHH3 and SHH4—The *SHH3* gene (*YMR118c*) was amplified from yeast genomic DNA by PCR as a 1-kb fragment with BamHI sites introduced at both ends. The fragment was cloned into the low copy centromeric plasmid YCplac33 and the high copy episomal plasmids YEplac181 and YEplac195 (25). Similarly, the *SHH4* gene (*YLR164w*) was amplified by PCR as a 0.9-kb fragment with EcoRI sites and cloned into YCplac33 and YEplac195. All cloned genes were sequenced in their entirety. The *TIM18* gene was cloned as a 1.2-kb EcoRI fragment from pOK94 (20) into YCplac33 and YEplac195.

Isolation of Submitochondrial Particles—Yeast precultures were grown on SD medium for 2 days to select for plasmid retention. YPGal medium was inoculated to a starting A_{600} of 0.1 and grown at 30 °C for 3 days. Cells were harvested, washed, and lysed in a French pressure cell (26). Mitochondrial membranes were isolated by differential centrifugation, resuspended in 20 mM HEPES-KOH, pH 7.4, flash frozen in liquid N_2, and stored at −80 °C.

Enzyme Assays and Kinetic Analysis—SDH is normally isolated partially inhibited by oxaloacetate. To activate it, membranes are preincubated in 20 mM succinate for 15 min at 30 °C immediately prior to assaying (27). The malonate-sensitive, succinate-dependent phenazine methosulfate (PMS)-mediated reduction of dichlorophenol indophenol (DCPIP) is used as a measure of membrane-associated catalytic dimer; this activity does not require a catalytically competent membrane domain. The malonate-sensitive, succinate-dependent reduction of quinone was monitored spectrophotometrically as the decylubiquinone (DB)-mediated reduction of DCPIP. Kinetic parameters for DB were determined by varying its concentration at fixed saturating concentrations of succinate and DCPIP. The

apparent K_m and V_{max} values were calculated from a non-linear regression fit of the data to the Michaelis-Menten equation using SigmaPlot 11.0 (Systat Software). SDH thermal stability was examined by incubating activated membrane fractions for 10 min at temperatures ranging from 30 to 65 °C and assaying for succinate-DB reductase activity. Malonate-sensitive, succinate-dependent cytochrome *c* reductase activity was measured as described (28). Values represent the mean of at least 15 measurements ±S.D. unless indicated.

Miscellaneous Methods—Measurements of covalent FAD content and protein concentration, yeast and *E. coli* transformations, and recombinant DNA methods have been described previously (26).

Preparation of Exometabolome Samples—Samples were prepared as described previously (23, 29). Cells were grown for 36 h at 30 °C in 2 ml of 2% yeast extract, 1% peptone, 0.25% glucose after which the optical density at 600 nm was measured. The remainder of the culture was centrifuged at 14,000 × *g* for 2 min. The clarified media were transferred to new microcentrifuge tubes and adjusted to 5% (w/v) trichloroacetic acid (TCA). Samples were incubated for 30 min on ice and centrifuged at 14,000 × *g* for 15 min at 4 °C. Supernatants were recovered, the pH was neutralized with NaOH, and samples were flash frozen. Samples were lyophilized for 2 days and stored at 4 °C with desiccant. About 50 mg of each lyophilized sample were dissolved in 570 μl of D_2O (99.9%; Isotec Inc., Miamisburg, OH); 30 μl of 5 mM 2,2-dimethyl-2-sila-3,3,4,4,5,5-hexadeuteropentane sulfonic acid (DSS-d_6; Chenomx Inc., Edmonton, Alberta, Canada) were added as a concentration standard and chemical shift indicator. The pH was recorded for calibration purposes, and residual particulate matter was removed by centrifugation at 14,000 × *g* for 3 min. 510 μl of supernatants were transferred to 5-mm-diameter NMR tubes for spectroscopic analysis.

^{1}H NMR Spectroscopy and NMR Data Processing—One-dimensional ^{1}H NMR spectra were acquired as described previously (23, 29). All spectra were acquired using transform NOESY pulse sequence (Vnmr 6.1B software, Varian Inc., Palo Alto, CA) on a 600-MHz Varian Inova spectrometer (Varian Inc.). The following conditions and parameters were used: 30 °C, 4-s acquisition time, 1-s preacquisition delay, 0.1-s mixing time, 7200-Hz sweep width, 7.95-μs pulse width, and 256 transients (23, 30). All spectra were Fourier transformed without applying line broadening, referenced to the DSS-d_6 standard, manually phased, and base line-corrected. Identification and quantification of metabolites were performed using Chenomx NMR Suite Professional software v5.1 (Chenomx Inc.).

Metabolite Data Analysis—To compare data between strains, we normalized the metabolite concentrations to the mass of lyophilized material and to the final optical densities of the respective cultures. To model and interpret metabolic data, multivariate analysis was performed using Simca P+ v12.0.1 software (Umetrics, Umeå, Sweden). Data were mean-centered and scaled to unit variance. Initial inspections of data were carried out using principal component analysis to identify potential outliers (data not shown). Subsequently, the data were subjected to partial least square discriminate analysis (PLS-DA), a supervised extension of principal component analysis, to obtain maximal discrimination between the strains (31). Model goodness of fit (R^2) and goodness or predictability (Q^2) values were determined for each model; the difference between the two values should not exceed 0.2 in a valid model (31). Permutation testing was also performed to assess model validity. Individual groups within each model were assessed by performing 999 random permutations of the *y* variables (strain) while keeping *x* variables (metabolites) intact. Randomly generated R^2 and Q^2 values were compared with the original model. Two features indicate that the models are valid. First, no permutations outperformed the original model (all permuted R^2 and Q^2 values are less than the points on the far right, which represent the original model). Second, the *y* intercepts for the R^2 and Q^2 regression line do not exceed 0.4 and 0.05, respectively (31). CV-ANOVA (analysis of variance testing of cross-validated predictive residuals) tests were performed to determine whether the differences between strains in each model were significant.

RESULTS

Comparison of Paralogs with Wild Type Subunits—Shh3p shows high sequence identity (57%) with Sdh3p (Fig. 1*A*), including the presence of three transmembrane segments predicted by TopPred (residues 96–118, 138–158, and 176–196) (32) and the presence of a mitochondrial targeting sequence predicted by MitoProt II (cleavage after residue 25, $p = 0.95$) (33). A quinone-binding site motif, L*XXX*H*XX*T (34, 35), and the histidine residue that functions as a heme axial ligand (His-156 in Sdh3p) are conserved (36). Previously, we have identified Sdh3p Ser-93, His-96, Arg-97, Phe-153, His-163, and Trp-166 as important for quinone reductase activity; all six of these residues are conserved in Shh3p (23, 26, 37). Ser-93 is the site of the *mev-1* mutation, which was isolated in *Caenorhabditis elegans* and confers hypersensitivity to oxidative stress and results in premature aging (38).

Similarly, the Shh4p and Tim18p paralogs show high sequence identity with Sdh4p (52 and 36%, respectively; Fig. 1*B*). TopPred predicts three transmembrane helices in both Shh4p (residues 66–86, 90–110, and 123–143) and Tim18p (residues 87–107, 112–132, and 144–164) (32). Both are predicted to have mitochondrial targeting sequences (Shh4p: cleavage after 32 amino acids, $p = 0.98$; Tim18p: cleavage after 43 amino acids, $p = 0.94$) (33). Three Sdh4p residues that we have previously proposed to be part of a distal quinone-binding site, Phe-100, Ser-102, and Lys-163, are conserved in Shh4p, but only the Ser and the Lys are found in Tim18p (27). Asp-119 and Tyr-120 are located in the proximal quinone-binding site, and both residues are found in all three proteins. Finally, Cys-109 is found in Sdh4p and Shh4p but not in Tim18p. We identified this residue as the axial ligand for the heme (36, 39, 40).

Growth Phenotypes—The high sequence identities between Sdh3p and Sdh4p and their respective paralogs prompted us to investigate whether the paralogs could function as authentic SDH subunits. We cloned *SHH3*, *SHH4*, and *TIM18* genes into single and multicopy vectors and transformed these plasmids into strains lacking *SDH3*, *SDH4*, or both *SDH3* and *SDH4.* The wild type *SDH3* gene in single copy but not the empty vector was able to restore respiratory growth on glycerol to a Δ*sdh3* mutant (Fig. 2*A*, *lanes 1* and *3*, respectively). *SHH3* was also able to restore comparable levels of respiratory growth when

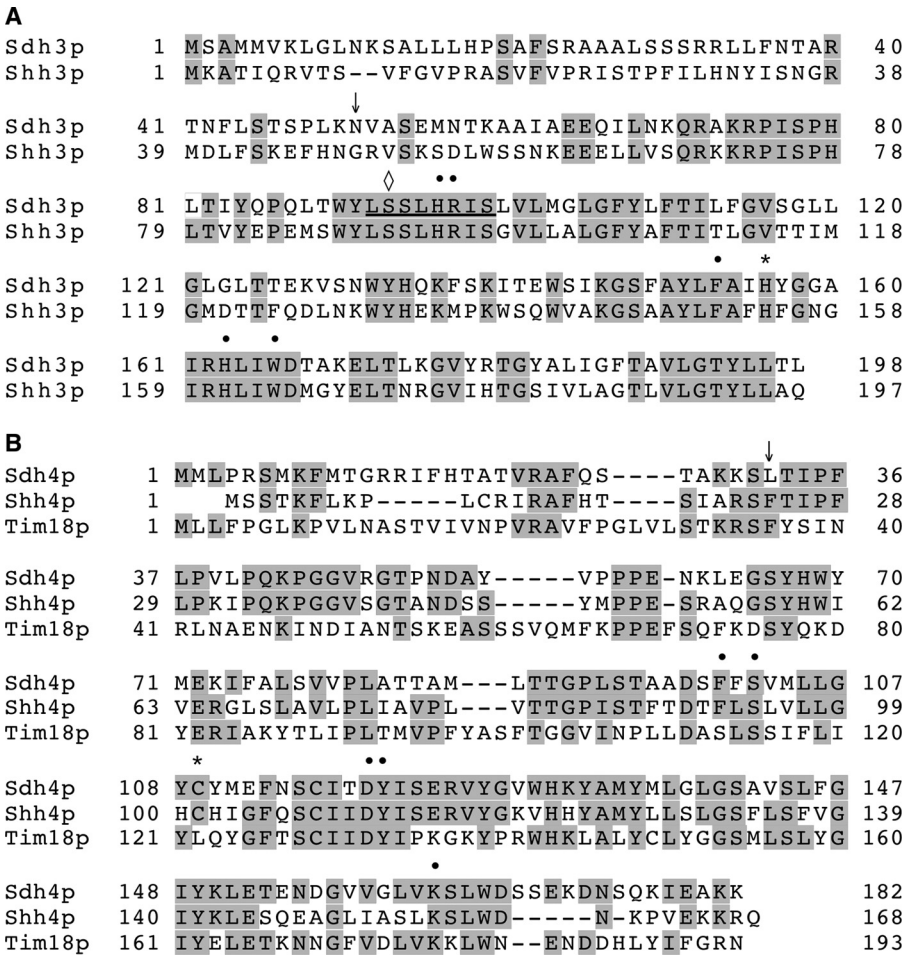

FIGURE 1. **Alignment of paralogs with wild type membrane anchor subunits.** *A*, the Sdh3p and Shh3p sequences (GenBank accession numbers CAA81982 and AAS56294, respectively) were aligned using ClustalW (71). Identical residues are *shaded*. The *arrow* identifies the first residue of mature Sdh3p after the mitochondrial targeting signal is removed (72). The *diamond* identifies Ser-93, the site of the *mev-1* mutation within the quinone-binding site motif (*underlined*). The *asterisk* is over His-156, an axial ligand for the heme b_{562} (36, 39, 40). The *black dots* are over Sdh3p residues identified previously to be important for quinone reductase activity. *B*, the Sdh4p, Shh4p, and Tim18p sequences (GenBank accession numbers CAA86683, AAB67488, and EEU07511, respectively) were aligned. The *arrow* identifies the first residue of mature Sdh4p after the mitochondrial targeting signal is removed. The *asterisk* is over Cys-109, an axial ligand for the heme b_{562} (36, 39, 40). The *black dots* are over Sdh4p residues identified previously to be important for quinone reductase activity.

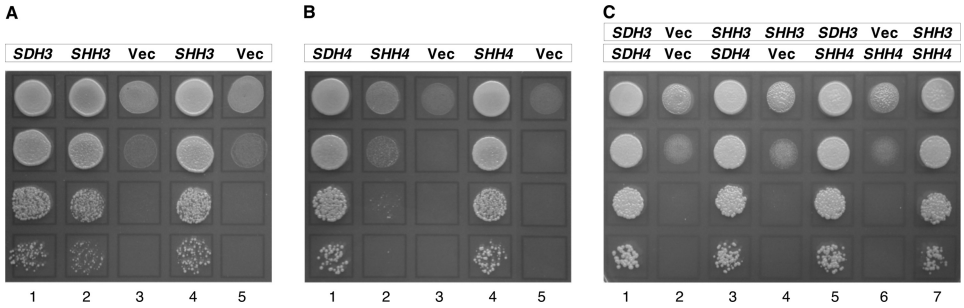

FIGURE 2. **Respiratory growth of wild type and paralog-expressing strains on glycerol.** Cultures were grown overnight at 30 °C in SD medium, serially diluted with sterile water, and spotted as 5-μl aliquots onto SG plates. Plates were incubated at 30 °C and photographed after 6 days. *A*, a Δ*sdh3* strain was transformed with *SDH3* on YCplac33 (*lane 1*), *SHH3* on YCplac33 (*lane 2*), the single copy vector (*Vec*) YCplac33 (*lane 3*), *SHH3* on YEplac195 (*lane 4*), and the multicopy vector YEplac195 (*lane 5*). *B*, a Δ*sdh4* strain was transformed with *SDH4* on YCplac33 (*lane 1*), *SHH4* on YCplac33 (*lane 2*), YCplac33 (*lane 3*), *SHH4* on YEplac195 (*lane 4*), and YEplac195 (*lane 5*). *C*, a Δ*sdh3* Δ*sdh4* strain was transformed with *SDH3* on YEplac181 and *SDH4* on YEplac195 (*lane 1*), YEplac181 and YEplac195 (*lane 2*), *SHH3* on YEplac181 and *SDH4* on YEplac195 (*lane 3*), *SHH3* on YEplac181 and YEplac195 (*lane 4*), *SDH3* on YEplac181 and *SHH4* on YEplac195 (*lane 5*), YEplac181 and *SHH4* on YEplac195 (*lane 6*), and *SHH3* on YEplac181 and *SHH4* on YEplac 195 (*lane 7*).

expressed from either single or multicopy vectors (Fig. 2*A*, *lanes 2* and *4*, respectively).

Similarly, the wild type *SDH4* restored respiratory growth on glycerol to a Δ*sdh4* mutant but not the empty vector (Fig. 2*B*, *lanes 1* and *3*, respectively). *SHH4* on a single copy vector supported slow growth but supported wild type growth when expressed from a multicopy plasmid (Fig. 2*B*, *lanes 2* and *4*, respectively). In contrast, *TIM18* was not able to support respiratory growth in a Δ*sdh4* strain when expressed from either single or multicopy vectors (data not shown).

TABLE 1
SDH assembly and activity in mitochondrial membranes

Strain	Covalent FAD[a]	PMS-DCPIP reductase activities	
		Specific activity[b]	Turnover number[c]
Δ*sdh3* + p*SDH3*	52 ± 2	230 ± 20	4400 ± 400
Δ*sdh3* + p*SHH3*	54.2 ± 0.5 (104%)[d]	240 ± 20 (104%)	4400 ± 300 (100%)
Δ*sdh3* + vector	ND[e]	12 ± 1 (5%)	
Δ*sdh4* + p*SDH4*	40 ± 1	189 ± 8	4800 ± 200
Δ*sdh4* + p*SHH4*	27.6 ± 0.8 (69%)	96 ± 9 (51%)	3500 ± 300 (73%)
Δ*sdh4* + vector	ND	10.6 ± 0.8 (6%)	
Δ*sdh3* Δ*sdh4* + p*SDH3* p*SDH4*	24.1 ± 0.8	92 ± 8	3800 ± 300
Δ*sdh3* Δ*sdh4* + p*SHH3* p*SHH4*	20.6 ± 0.2 (85%)	56 ± 6 (61%)	2700 ± 300 (71%)
Δ*sdh3* Δ*sdh4* + vectors	9.7 ± 0.6 (40%)	7 ± 1 (8%)	700 ± 100 (18%)
Δ*sdh3* Δ*sdh4* Δ*shh3*	8.2 ± 0.5 (34%)	6.7 ± 0.4 (7%)	820 ± 60 (22%)

[a] FAD contents are expressed as pmol of FAD mg of protein^{-1}. Values represent the mean of three trials ±S.D.
[b] Expressed as nmol of PMS-mediated DCPIP reduced min^{-1} mg of protein^{-1}.
[c] Expressed as μmol of PMS-mediated DCPIP reduced min^{-1} μmol of covalent FAD^{-1}.
[d] Values in parentheses represent the percent activities of the hybrid enzymes compared with their respective wild type controls.
[e] ND, not detectable.

TABLE 2
Quinone-mediated activities of SDH enzymes in mitochondrial membranes

Strain	Cytochrome *c* reductase		Decylubiquinone reductase	
	Specific activity[a]	Turnover number[b]	Specific activity[c]	Turnover number[d]
Δ*sdh3* + p*SDH3*	113 ± 7	2200 ± 200	220 ± 10	4200 ± 300
Δ*sdh3* + p*SHH3*	77 ± 7 (68%)[e]	1400 ± 100 (64%)	131 ± 8 (60%)	2400 ± 100 (57%)
Δ*sdh3* + vector	3 ± 2 (3%)		2.1 ± 0.5 (1%)	
Δ*sdh4* + p*SDH4*	86 ± 8	2200 ± 200	182 ± 9	4500 ± 300
Δ*sdh4* + p*SHH4*	19 ± 1 (22%)	690 ± 50 (30%)	28 ± 3 (15%)	1010 ± 80 (22%)
Δ*sdh4* + vector	2.5 ± 0.9 (3%)		2.7 ± 0.5 (1%)	
Δ*sdh3* Δ*sdh4* + p*SDH3* p*SDH4*	65 ± 5	2700 ± 200	83 ± 5	3500 ± 200
Δ*sdh3* Δ*sdh4* + p*SHH3* p*SHH4*	33 ± 2 (51%)	1600 ± 100 (60%)	34 ± 4 (41%)	1700 ± 200 (49%)
Δ*sdh3* Δ*sdh4* + vectors	2.0 ± 0.9 (3%)	210 ± 90 (8%)	3.3 ± 0.7 (4%)	330 ± 70 (9%)
Δ*sdh3* Δ*sdh4* Δ*shh3*	ND[f]		1.7 ± 0.8 (2%)	200 ± 100 (6%)

[a] Expressed as nmol of cytochrome *c* reduced min^{-1} mg of protein^{-1}.
[b] Expressed as μmol of cytochrome *c* reduced min^{-1} μmol of covalent FAD^{-1}.
[c] Expressed as nmol of DB-mediated DCPIP reduced min^{-1} mg of protein^{-1}.
[d] Expressed as μmol of DB-mediated DCPIP reduced min^{-1} μmol of covalent FAD^{-1}.
[e] Values in parentheses represent the percent activities of the hybrid enzymes compared with their respective wild type controls.
[f] Not detectable.

We constructed a strain lacking both *SDH3* and *SDH4* to determine whether *SHH3* and *SHH4* together could lead to the expression of a functional SDH. As expected, the *SDH3* and *SDH4* genes together were capable of restoring respiratory growth (Fig. 2*C*, *lanes 1* and *2*). The combinations involving one authentic SDH subunit and one paralog also resulted in growth (Fig. 2*C*, *lanes 3–6*). Finally, *SHH3* and *SHH4* together were able to support growth that was only slightly reduced compared with when the authentic SDH genes were used (Fig. 2*C*, *lane 7*). Therefore, we conclude that *Shh3p* and *Shh4p* are functional *in vivo* when expressed with either an authentic SDH subunit partner or with each other.

Hybrid Enzymes Are Catalytically Competent—We determined the amounts of covalent FAD in crude mitochondrial preparations. SDH is the major covalent flavoprotein in *S. cerevisiae*, and the levels of TCA-precipitable flavin are a measure of SDH levels (28). All hybrid enzymes were efficiently produced with FAD contents ranging between 69 and 104% of the strains expressing the corresponding wild type SDH genes (Table 1). We also determined the succinate-dependent, PMS-mediated DCPIP reductase activity in mitochondrial membranes as a measure of enzyme assembly. This activity is a measure of the membrane-associated catalytic dimer; it does not require catalytically competent membrane subunits, but the subunits must be able to mediate membrane association of the Sdh1p/Sdh2p catalytic dimer (41, 42). *SHH3* and *SHH4* expression resulted in turnover numbers of 100 and 73% of wild type for DCPIP reductase activity, respectively (Table 1). When both *SHH3* and *SHH4* were expressed together, 71% activity was measured. These results indicate that the hybrid enzymes are efficiently inserted into the membrane. Cytochrome *c* and DB reductase activities both require a functional membrane domain. The hybrid enzyme containing Shh3p was able to efficiently catalyze both activities with 64 and 57%, respectively, of the wild type activities (Table 2). The hybrid enzyme containing Shh4p was less efficient with 30 and 23%, respectively, of wild type activities. Interestingly, the hybrid enzyme containing both Shh3p and Shh4p was more active (60 and 49%, respectively) than the enzyme containing Shh4p only. These results are consistent with the growth phenotypes we observed and confirm that hybrid SDH enzymes are catalytically competent *in vivo* and *in vitro*.

It should be noted that the strain background used to create the Δ*sdh3* Δ*sdh4* double mutant (YPH499) is different from the single mutant strains (MH125). As reported previously, SDH gene disruption strains in a YPH499 background have higher levels of residual covalent FAD and SDH enzymatic activities (43). One possible explanation is that in the absence of the wild type subunits the expression of the paralogs is being induced in this strain background. However, their expression is presumed

TABLE 3
Apparent kinetic parameters for decylubiquinone reductase activities of wild type and hybrid SDH enzymes in mitochondrial membranes

Strain	K_m [a,b]	V_{max} [c]	k_{cat} [d]	k_{cat}/K_m [e]
Δ*sdh3* + p*SDH3*	3.4 ± 0.3	219 ± 5	4200 ± 200	1.2×10^3
Δ*sdh3* + p*SHH3*	2.7 ± 0.2	132 ± 3	2410 ± 60	8.9×10^2
Δ*sdh4* + p*SDH4*	2.9 ± 0.1	183 ± 2	4600 ± 100	1.6×10^3
Δ*sdh4* + p*SHH4*	2.1 ± 0.3	23.2 ± 0.8	910 ± 30	4.3×10^2
Δ*sdh3* Δ*sdh4* + p*SDH3* p*SDH4*	2.8 ± 0.1	81.5 ± 0.8	3500 ± 100	1.3×10^3
Δ*sdh3* Δ*sdh4* + p*SHH3* p*SHH4*	1.8 ± 0.2	33.5 ± 0.9	1620 ± 40	9.0×10^2

[a] Each value represents the mean of six measurements ±S.E.
[b] Values are expressed in μM.
[c] Activities are expressed as nmol of DB-mediated DCPIP reduced min^{-1} mg of $protein^{-1}$.
[d] Values are expressed as μmol of DB-mediated DCPIP reduced min^{-1} μmol of covalent FAD^{-1}.
[e] Values are expressed as μM^{-1} min^{-1}.

to be low as it was not significant enough to confer respiration competence (Fig. 2). To examine this possibility, a Δ*sdh3* Δ*sdh4* Δ*shh3* triple deletion strain was generated. With the loss of three of the four membrane anchor subunit genes, potential assembly of any intact SDH enzyme would be abrogated. When this strain was examined, the FAD content and enzymatic activities decreased slightly, suggesting that there is some contribution from this effect. However, the majority of the residual activity in the YPH499 background does not appear to be related to SDH.

We determined whether the hybrid SDH enzymes displayed altered kinetic parameters for quinone reduction. The apparent K_m values for DB differed by less than 2-fold for the hybrid enzymes compared with wild type SDH (Table 3). The ratio k_{cat}/K_m (the rate constant for the reaction of free enzyme with free substrate to give product) is a measure of enzyme efficiency. The Shh3p and the double hybrid Shh3p-Shh4p enzymes were 74 and 69% as efficient as the wild type (Table 3). The Shh4p-containing enzyme, which showed the largest decrease in V_{max}, was the least efficient at 27% of the wild type.

We measured the stabilities of the wild type and hybrid enzymes at elevated temperatures to determine whether the altered membrane domains resulted in structural perturbation. All three hybrid enzymes were more sensitive to thermal denaturation than the wild type (Fig. 3). The Shh4p-containing SDH displayed the fastest loss of activity at the lower temperatures tested, but all enzymes were similarly sensitive at the highest temperatures. The decreases in stability are similar to some of the stability changes we have seen previously with single amino acid substitutions (27).

Hybrid Enzymes Create Distinct Metabotypes—The mitochondrial respiratory chain is central to cellular metabolic pathways not intimately associated with energy metabolism (44). Supporting this notion, we have reported previously that single amino acid mutations in SDH resulted in significant metabolic changes as reflected in the extracellular metabolome (exometabolome); we also found that the metabolic phenotypes or metabotypes were correlated with phenotypic analysis (29). To examine the metabolic consequences resulting from the expression of the hybrid enzymes, we characterized the exometabolomes of the various strains. We focused on the exometabolome because it is noninvasive while directly reflecting intracellular metabolic activity (45). We identified and quantified 30 acid-soluble metabolites in spent culture media using ^1H NMR spectroscopy. We used PLS-DA to model and analyze metabolomic data. The resulting PLS-DA scatter plots show

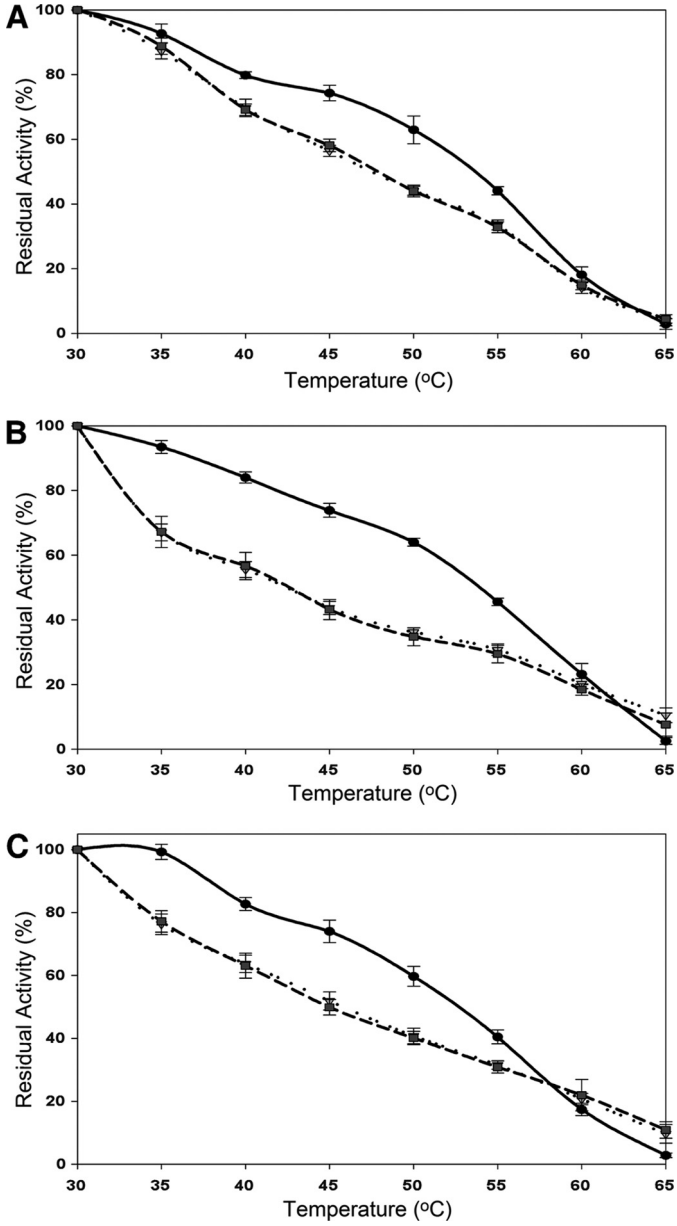

FIGURE 3. **Thermal stability of wild type and hybrid enzymes.** Membranes were preincubated in 20 mM succinate for 15 min at 30 °C prior to shifting to higher temperatures. Activated membrane fractions were incubated for 10 min at different temperatures and assayed for succinate-DB reductase activity. In each experiment, membranes containing the wild type enzyme were used as control (*solid curves*). Values represent the mean of at least three trials ±S.D. *Dashed curves* show membranes containing Shh3p and Sdh4p (*A*), Sdh3p and Shh4p (*B*), and Shh3p and Shh4p (*C*).

that the replicate data sets for the wild type and corresponding paralog-expressing strains can be discriminated and cluster into discernible groups (Fig. 4). Their locations are distinct from one another but reside in the same region of the scatter plot opposite to the deletion strain along component 1. Permutation testing indicated the validity of all three models (supplemental Fig. 1).

To further examine the metabolic differences between wild type and paralog-expressing strains, we performed PLS-DA without the respective knock-out strains (supplemental Fig. 2); permutation testing was also performed for these models (supplemental Fig. 3). All paralog-expressing strains can be discriminated from their wild type counterparts based on the exometabolomes. Metabolites that were significantly different based on Student's *t* test between respective wild type and hybrid strains are presented in Table 4. The same metabolites were also determined to contribute most highly to the discrimination in the PLS-DA models (supplemental Table I). Three metabolites were found to be univariately significant and important in model generation in all three strain sets: fumarate, isobutyrate, and succinate. Complete metabolomic data sets are presented in supplemental Tables II–IV.

DISCUSSION

The most distinguishing features of the SDH and fumarate reductase family of enzymes reside in the membrane domain. This domain can be composed of one or two polypeptides and can contain zero, one, or two hemes and one or two quinone-binding sites (13, 46). Here, we show that the yeast SDH can be assembled with paralogous subunits in its membrane domain, further increasing the structural complexity of this enzyme family.

Both of the Shh3p and Shh4p paralogs share considerable sequence identity with their respective authentic SDH subunits. In addition, they have retained amino acids that have been identified previously as functionally important. It is therefore not unexpected that Shh3p and Shh4p can effectively substitute for Sdh3p and Sdh4p, respectively, and form hybrid enzymes. Tim18p was not able to substitute for Sdh4p, and it lacks the proposed heme ligand corresponding to Cys-109 of Sdh4p (Fig. 1*B*). However, we and others have reported that the heme is not essential for SDH activity in *E. coli* (47) or in yeast (40). Nevertheless, it would be interesting to introduce a Cys residue into Tim18p to further investigate this issue. In Shh4p, Cys-102 is flanked by two histidines. Histidines are the most common axial ligands for hemes, and it would be interesting to determine whether either of these histidines can replace Cys-102 as the axial ligand.

The *S. cerevisiae* genome arose by whole genome duplication followed by a massive loss of genes (48). Over 450 duplicated gene pairs remain, including the *SDH3*/*SHH3* and *SDH4*/*SHH4* pairs. In about 17% of the duplicated gene pairs, one or both of the *S. cerevisiae* paralogs show accelerated protein evolution compared with the *Kluyveromyces waltii* homolog; *K. waltii* is a related yeast species that diverged before the genome duplication (48). It has been inferred that the slowly evolving paralogs probably retain their ancestral function, whereas the more rapidly evolving paralogs probably acquire new functions. Neither Shh3p nor Shh4p is a rapidly evolving protein, suggesting they may have retained their ancestral functions (48). This is consistent with their ability to complement Δ*sdh3* and Δ*sdh4* mutants, respectively (Fig. 2). In contrast, Tim18p has lost the ability to complement a Δ*sdh4* mutant and is now involved in mitochondrial protein import.

Do the paralog-containing hybrid enzymes contain heme? Previously, we and others measured the presence of heme in the *S. cerevisiae* enzyme by detecting a fumarate-oxidized, dithionite-reduced absorption peak at 562 nm (36, 49–51). Recently, this approach was questioned because fumarate oxidation of dithionite-reduced mitochondrial membranes might also reoxidize cytochromes in the ubiquinol-cytochrome *c* oxidoreductase (complex III) (52). These authors failed to detect a fumarate-oxidizable peak at 562 nm when atpenin A5 or when antimycin plus myxothiazol were added. Atpenin A5 is a quinone analog that binds at the proximal quinone-binding site and specifically inhibits SDH (53, 54); that it prevents the oxidation of the heme by fumarate is not surprising because in *E. coli* the quinone-binding site is required for electron transfer between the heme and the catalytic subunits (55). It is more difficult to explain the effects of the complex III inhibitors antimycin and myxothiazol, both of which are highly specific for complex III. However, to our knowledge, the only fumarate-oxidizable cytochromes reported are associated with SDH. Furthermore, some mutations in the cytochrome *b* subunit of complex III, such as W142R, can severely impair SDH activity (50). Trp-142 is within 5 Å of the quinone-binding site to which myxothiazol binds, and we speculate that myxothiazol binding might similarly impair SDH functions. New approaches are needed to unambiguously determine whether the wild type yeast SDH and the hybrid SDH enzymes contain heme. The presence of heme in the yeast SDH has been questioned because it does not possess the canonical axial histidine ligands for the heme. The histidine in Sdh4p is replaced by a cysteine at the corresponding position (Cys-109). Although this situation is not highly prevalent, it is not unique. The *Trypanosoma cruzi* SDH enzyme was recently purified and shown to contain heme, but the histidine ligand in the SDH3 subunit is absent (56). In addition, in rice SDH4 (GenBank™ accession number NP_001045324) and in *Trypanosoma brucei* SDH4, the heme ligand His residue is substituted by Gln (56).

It is worth noting that the hybrid enzyme containing both Shh3p and Shh4p was more active than the hybrid enzyme containing Sdh3p and Shh4p (Tables 1 and 2). This suggests that the structural mismatch between Sdh3p and Shh4p is more severe than any mismatch between Shh3p and Shh4p. This conjecture is also supported by the thermal denaturation data in which the Shh4p hybrid enzyme was less stable than the double hybrid. These observations might suggest that Shh3p and Shh4p have co-evolved to form a double hybrid enzyme rather than function in single hybrid enzymes. If this were the case, it would also be expected that these two genes would be co-expressed.

To investigate whether the paralogs are co-expressed, we examined the expression of SDH-related genes in several microarray data sets (Fig. 5). These data sets include changes in expression during the unfolded protein response (57), histone

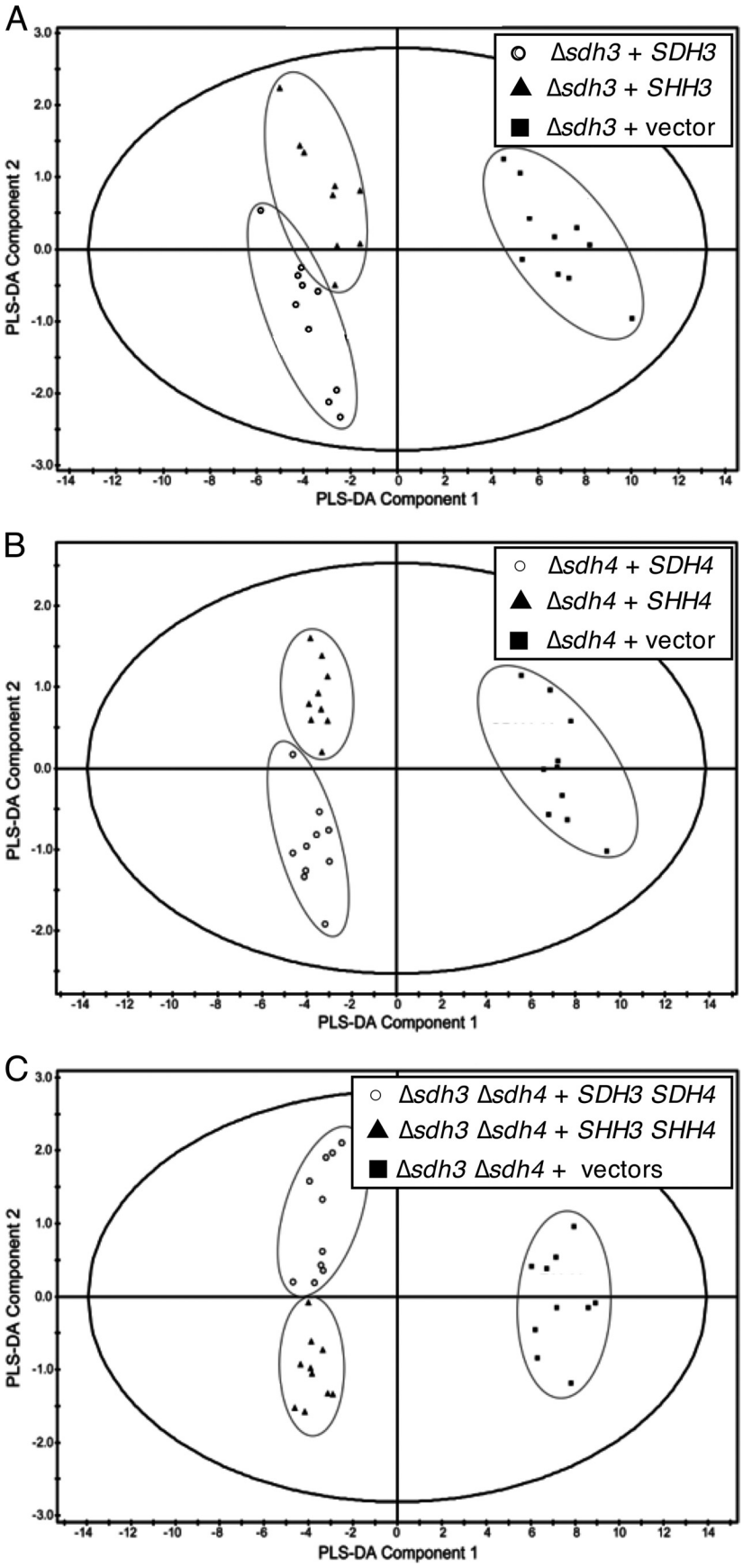
A
Δsdh3 + SDH3
Δsdh3 + SHH3
Δsdh3 + vector
PLS-DA Component 2
PLS-DA Component 1
B
Δsdh4 + SDH4
Δsdh4 + SHH4
Δsdh4 + vector
PLS-DA Component 2
PLS-DA Component 1
C
Δsdh3 Δsdh4 + SDH3 SDH4
Δsdh3 Δsdh4 + SHH3 SHH4
Δsdh3 Δsdh4 + vectors
PLS-DA Component 2
PLS-DA Component 1

TABLE 4
Extracellular metabolites significantly different between wild type and paralog-expressing strains

	Δ*sdh3*			Δ*sdh4*			Δ*sdh3* Δ*sdh4*		
	+p*SDH3*	+p*SHH3*	*p* value	+p*SDH4*	+p*SHH4*	*p* value	+p*SDH3* p*SDH4*	+p*SHH3* p*SHH4*	*p* value
Arg	1865.0 ± 227.1	1931.9 ± 174.6		1778.1 ± 139.5	1888.5 ± 85.0	<0.05	1772.2 ± 121.3	1790.1 ± 132.8	
Asn	142.1 ± 12.4	169.1 ± 43.4		180.2 ± 27.9	259.6 ± 22.0	<0.001	311.6 ± 44.8	393.2 ± 58.3	<0.01
Asp	913.1 ± 95.6	896.3 ± 89.1		847.7 ± 78.0	830.6 ± 48.8		959.9 ± 67.2	863.2 ± 71.8	<0.01
Fumarate	5.4 ± 0.8	4.4 ± 0.6	<0.01	5.3 ± 0.4	4.3 ± 0.3	<0.001	7.6 ± 1.0	5.4 ± 0.5	<0.001
Glycerol	284.4 ± 42.8	291.0 ± 77.0		266.7 ± 22.0	270.5 ± 44.2		316.0 ± 28.4	361.4 ± 40.0	<0.01
Gly	1706.6 ± 112.8	1743.4 ± 115.0		1639.1 ± 123.6	1608.0 ± 48.0		1810.4 ± 104.1	1673.4 ± 98.2	<0.01
Isobutyrate	56.3 ± 3.1	49.5 ± 5.1	<0.01	52.1 ± 4.5	45.5 ± 2.5	<0.01	37.5 ± 3.9	33.0 ± 2.3	<0.01
Ile	1221.9 ± 115.4	1328.7 ± 106.6	<0.05	1222.1 ± 96.3	1241.1 ± 50.2		1313.8 ± 79.2	1249.6 ± 87.6	
Lactate	41.5 ± 8.3	50.1 ± 9.2	<0.05	31.1 ± 5.5	32.7 ± 3.5		36.5 ± 5.9	41.8 ± 6.8	
Lys	1180.8 ± 81.3	1226.7 ± 113.1		1090.9 ± 80.7	1117.1 ± 41.5		1312.0 ± 103.3	1200.7 ± 92.6	<0.05
Phe	719.1 ± 44.0	845.8 ± 84.5	<0.001	776.2 ± 64.3	861.3 ± 43.2	<0.01	1048.7 ± 69.2	1028.6 ± 75.7	
Ser	691.4 ± 76.0	714.7 ± 135.4		650.6 ± 83.3	749.5 ± 45.4	<0.01	1021.8 ± 106.9	897.4 ± 82.8	<0.01
Succinate	308.6 ± 26.3	411.4 ± 39.6	<0.001	371.8 ± 42.9	432.9 ± 34.4	<0.01	474.5 ± 33.3	550.7 ± 100.8	<0.05
Thr	447.9 ± 47.2	445.7 ± 61.0		405.3 ± 28.4	465.7 ± 36.6	<0.001	702.5 ± 43.5	631.6 ± 27.1	<0.001
Tyr	321.9 ± 24.6	351.6 ± 28.4	<0.05	309.1 ± 27.0	326.4 ± 12.5		395.8 ± 28.9	381.5 ± 28.6	
Uracil	50.3 ± 3.7	54.0 ± 6.2		47.6 ± 3.4	44.5 ± 5.5		48.7 ± 4.5	35.5 ± 2.0	<0.001

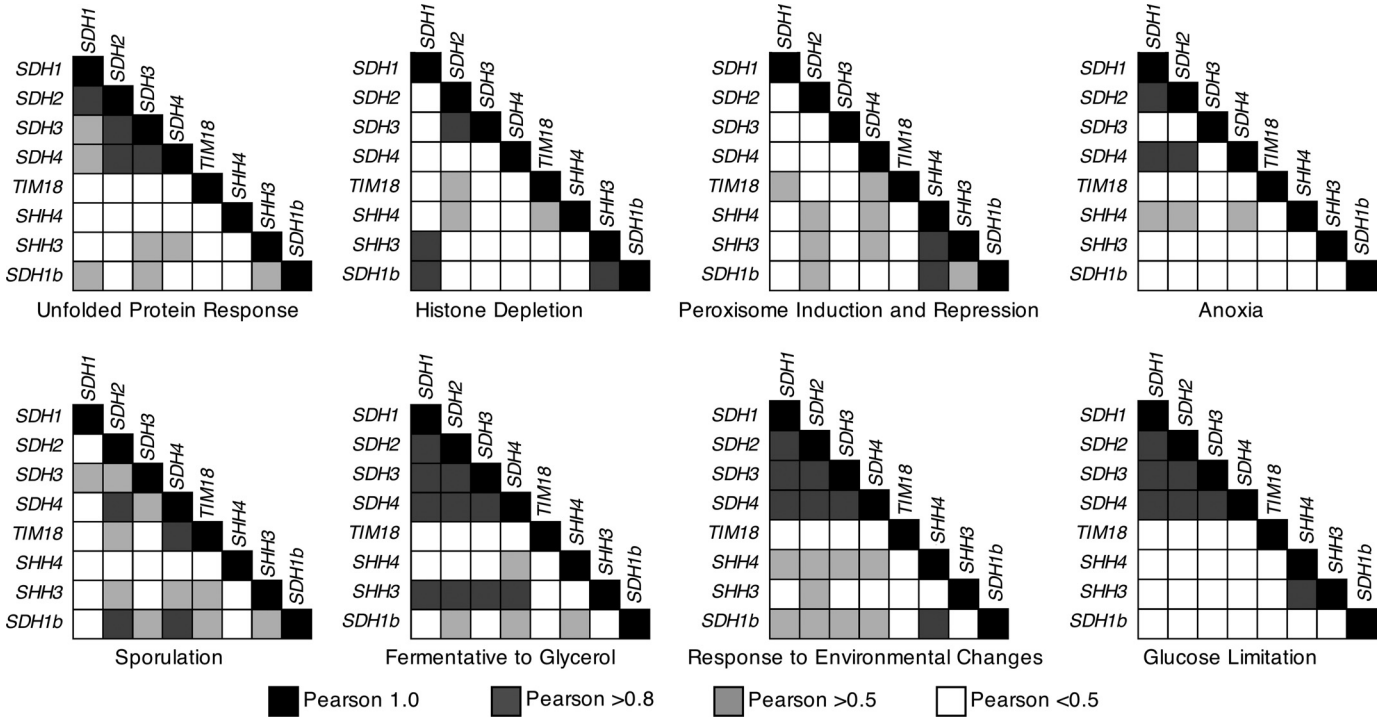

FIGURE 5. **Transcriptional expression of SDH genes.** Several expression data sets deposited in the *Saccharomyces* Genome Database were compared using Expression Connection for the similarities of expression for the eight SDH-related genes. The Pearson correlation is a statistical measure of how similar the expression of two gene products is. A Pearson coefficient of 1.0 is a perfect correlation. The "response to environmental changes" data set includes heat shock, osmotic stress, oxidative stress, amino acid starvation, nitrogen depletion, the diauxic shift, transition to stationary phase, and growth on a variety of carbohydrates.

depletion (58), peroxisome induction and repression (59), anoxia and reoxygenation (60), sporulation (61), fermentative to glycerol transition (62), response to environmental changes (63), and glucose limitation (64). As would be expected from genes expressing subunits of an enzyme involved in energy metabolism, the expression profiles of the *SDH1*, *SDH2*, *SDH3*, and *SDH4* genes are highly correlated (Pearson coefficients >0.8) in the glucose limitation, response to environmental changes, and the fermentative to glycerol transition data sets. The expression of these genes is also somewhat correlated during the unfolded protein response. In contrast, the expression of *TIM18* only achieves a strong correlation with the *SDH4* gene in the sporulation data set, strongly indicating that the primary role of Tim18p is not in energy metabolism.

The expression profiles of *SHH3* and *SHH4* are highly correlated in the peroxisome induction and repression and the glu-

FIGURE 4. **PLS-DA model plots of exometabolome profiles.** Each *dot* represents one replicate metabotype. *A*, the Δ*sdh3* mutant strain was transformed with *SDH3* (*circles*), *SHH3* (*filled triangles*), or empty vector (*filled squares*). R^2X, 0.922; R^2Y, 0.823; Q^2, 0.755; CV-ANOVA, 2.18×10^{-5}. *B*, the Δ*sdh4* mutant strain was transformed with *SDH4* (*circles*), *SHH4* (*filled triangles*), or empty vector (*filled squares*). R^2X, 0.952; R^2Y, 0.826; Q^2, 0.802; CV-ANOVA, 2.24×10^{-6}. *C*, the Δ*sdh3* Δ*sdh4* mutant strain was transformed with *SDH3* and *SDH4* (*circles*), *SHH3* and *SHH4* (*filled triangles*), or empty vectors (*filled squares*). R^2X, 0.973; R^2Y, 0.820; Q^2, 0.804; CV-ANOVA, 6.05×10^{-5}.

cose limitation data sets but are not correlated in any other data set. This suggests that Shh3p and Shh4p are not always co-expressed and that a double hybrid SDH may only be present under select conditions. Interestingly, *SHH3*, *SHH4*, and *SDH1b* expression profiles are highly correlated in the peroxisome induction and repression data set. In this data set, expression of *SDH2* is also correlated but more weakly with these three genes. This suggests that conditions that induce and repress peroxisomes might lead to the assembly of an SDH enzyme composed of Sdh1bp, Sdh2p, Shh3p, and Shh4p. One of the functions of peroxisomes and the glyoxylate cycle localized there is the formation of succinate, an SDH substrate.

The expression of *SDH1b* is strongly correlated with *SDH2* and *SDH4* expression and more weakly correlated with *SDH3* expression in the sporulation data set. This may suggest a role for an Sdh1bp-containing enzyme in sporulation and nitrogen depletion. The expression of *SHH3* is also highly correlated with all four SDH genes in the fermentative to glycerol transition data set.

The yeast mitochondrial proteome has been thoroughly investigated, and ~90% of all mitochondrial proteins have been detected (65). Highly purified mitochondria isolated from the strain YPH499 grown under respiratory conditions on a rich glycerol medium (YPG) contain all of the proteins discussed here (Sdh1p, Sdh2p, Sdh3p, Sdh4p, Sdh1bp, Shh4p, and Tim18p) except Shh3p. Shh3p may not have been detected because it is not expressed, although its mRNA is present under these conditions. However, post-transcriptional regulation may have prevented its translation. Alternatively, Shh3p may have escaped detection by the separation and detection methods used (65). However, Shh3p was detected by mass spectrometry when expressed from its natural chromosomal location as a tagged protein; these studies were performed in cultures grown in rich glucose medium (66).

The microarray data sets suggest that alternative forms of SDH may also be assembled under more restrictive conditions. Proteomics studies under these more restrictive conditions will be needed to confirm their expression. Under respiratory conditions, Shh3p and Shh4p can assemble with authentic SDH subunits to produce hybrid enzymes with altered metabolic properties as demonstrated by their different exometabotypes. Although PLS-DA revealed that hybrid strains produced distinctly different metabotypes from wild type strains, it also revealed that the hybrid metabotypes much more closely resemble wild type stains than deletion strains. Indeed, hybrid strains failed to secrete acetate, a marker that we reported previously to be associated with loss of enzyme function (29).

Although hybrid enzymes likely play a role in responding to restrictive environmental conditions, they may also provide advantages for present day industrial purposes. Organic molecules produced by yeast strains, including *S. cerevisiae*, during fermentation are considered to be important flavor components of wine (67). For example, succinate is considered to be an important flavor component of sake, and yeast strains that produce higher quantities of succinate are favored (68). A variety of fusel alcohols, such as 2- and 3-methyl butanol, 2-methyl propanol, and phenylethyl alcohol, produced during the fermentation of amino acids are also considered to be important flavor compounds (67). Conversely, the fusel alcohol isobutanol produced from isobutyrate is thought to contribute to wine spoilage (69, 70). Interestingly, the strains expressing the paralog subunits produce both more succinate and less isobutyrate than their wild type counterparts (Table 4). Unfortunately, we were not able to quantify fusel alcohols using ^{1}H NMR spectroscopy.

In summary, we have cloned and expressed two SDH paralogs and created hybrid enzymes. Shh3p and Shh4p can singly or together form functional membrane-bound isoenzymes of succinate dehydrogenase. The isoenzymes have significant levels of quinone reduction activity *in vivo* and *in vitro*. Alternative forms of SDH containing one or more paralogous subunits are likely produced during respiratory growth on glycerol and possibly under non-optimal growth conditions. The alternative forms of SDH alter the kinetic properties of the enzyme and the global metabolic state and may provide growth advantages. Surprisingly, Sdh3p can form SDH enzymes in complex with Sdh4p or Shh4p or it can enter the TIM22 translocase in complex with Tim18p.

Acknowledgment—We thank Dr. Rob Jensen for the TIM18 plasmid.

REFERENCES

1. Lemire, B. D., and Oyedotun, K. S. (2002) The *Saccharomyces cerevisiae* mitochondrial succinate:ubiquinone oxidoreductase. *Biochim. Biophys. Acta* **1553,** 102–116
2. Bardella, C., Pollard, P. J., and Tomlinson, I. (2011) SDH mutations in cancer. *Biochim. Biophys. Acta* **1807,** 1432–1443
3. Brière, J. J., Favier, J., El Ghouzzi, V., Djouadi, F., Bénit, P., Gimenez, A. P., and Rustin, P. (2005) Succinate dehydrogenase deficiency in human. *Cell. Mol. Life Sci.* **62,** 2317–2324
4. Eng, C., Kiuru, M., Fernandez, M. J., and Aaltonen, L. A. (2003) A role for mitochondrial enzymes in inherited neoplasia and beyond. *Nat. Rev. Cancer* **3,** 193–202
5. Gottlieb, E., and Tomlinson, I. P. (2005) Mitochondrial tumour suppressors: a genetic and biochemical update. *Nat. Rev. Cancer* **5,** 857–866
6. Rutter, J., Winge, D. R., and Schiffman, J. D. (2010) Succinate dehydrogenase—assembly, regulation and role in human disease. *Mitochondrion* **10,** 393–401
7. Burnichon, N., Brire, J. J., Lib, R., Vescovo, L., Rivire, J., Tissier, F., Jouanno, E., Jeunemaitre, X., Bnit, P., Tzagoloff, A., Rustin, P., Bertherat, J., Favier, J., and Gimenez-Roqueplo, A. P. (2010) SDHA is a tumor suppressor gene causing paraganglioma. *Hum. Mol. Genet.* **19,** 3011–3020
8. Pasini, B., McWhinney, S. R., Bei, T., Matyakhina, L., Stergiopoulos, S., Muchow, M., Boikos, S. A., Ferrando, B., Pacak, K., Assie, G., Baudin, E., Chompret, A., Ellison, J. W., Briere, J. J., Rustin, P., Gimenez-Roqueplo, A. P., Eng, C., Carney, J. A., and Stratakis, C. A. (2008) Clinical and molecular genetics of patients with the Carney-Stratakis syndrome and germline mutations of the genes coding for the succinate dehydrogenase subunits SDHB, SDHC, and SDHD. *Eur. J. Hum. Genet.* **16,** 79–88
9. Schimke, R. N., Collins, D. L., and Stolle, C. A. (2010) Paraganglioma, neuroblastoma, and a SDHB mutation: resolution of a 30-year-old mystery. *Am. J. Med. Genet. A* **152A,** 1531–1535
10. Albayrak, T., Scherhammer, V., Schoenfeld, N., Braziulis, E., Mund, T., Bauer, M. K., Scheffler, I. E., and Grimm, S. (2003) The tumor suppressor cybL, a component of the respiratory chain, mediates apoptosis induction. *Mol. Biol. Cell* **14,** 3082–3096
11. Ishii, T., Yasuda, K., Akatsuka, A., Hino, O., Hartman, P. S., and Ishii, N. (2005) A mutation in the SDHC gene of complex II increases oxidative stress, resulting in apoptosis and tumorigenesis. *Cancer Res.* **65,** 203–209
12. Lee, S., Nakamura, E., Yang, H., Wei, W., Linggi, M. S., Sajan, M. P., Farese, R. V., Freeman, R. S., Carter, B. D., Kaelin, W. G., Jr., and Schlisio, S. (2005)

Neuronal apoptosis linked to EglN3 prolyl hydroxylase and familial pheochromocytoma genes: developmental culling and cancer. *Cancer Cell* **8,** 155–167
13. Lancaster, C. R. (2002) Succinate:quinone oxidoreductases: an overview. *Biochim. Biophys. Acta* **1553,** 1–6
14. Cole, S. T., Condon, C., Lemire, B. D., and Weiner, J. H. (1985) Molecular biology, biochemistry and bioenergetics of fumarate reductase, a complex membrane-bound iron-sulfur flavoenzyme of *Escherichia coli*. *Biochim. Biophys. Acta* **811,** 381–403
15. Hederstedt, L. (1999) Respiration without O_2. *Science* **284,** 1941–1942
16. Iwata, F., Shinjyo, N., Amino, H., Sakamoto, K., Islam, M. K., Tsuji, N., and Kita, K. (2008) Change of subunit composition of mitochondrial complex II (succinate-ubiquinone reductase/quinol-fumarate reductase) in *Ascaris suum* during the migration in the experimental host. *Parasitol. Int.* **57,** 54–61
17. Roos, M. H., and Tielens, A. G. (1994) Differential expression of two succinate dehydrogenase subunit-B genes and a transition in energy metabolism during the development of the parasitic nematode *Haemonchus contortus*. *Mol. Biochem. Parasitol.* **66,** 273–281
18. Elorza, A., Roschzttardtz, H., Gómez, I., Mouras, A., Holuigue, L., Araya, A., and Jordana, X. (2006) A nuclear gene for the iron-sulfur subunit of mitochondrial complex II is specifically expressed during *Arabidopsis* seed development and germination. *Plant Cell Physiol.* **47,** 14–21
19. Colby, G., Ishii, Y., and Tzagoloff, A. (1998) Suppression of sdh1 mutations by the SDH1b gene of *Saccharomyces cerevisiae*. *Yeast* **14,** 1001–1006
20. Kerscher, O., Sepuri, N. B., and Jensen, R. E. (2000) Tim18p is a new component of the Tim54p-Tim22p translocon in the mitochondrial inner membrane. *Mol. Biol. Cell* **11,** 103–116
21. Koehler, C. M., Murphy, M. P., Bally, N. A., Leuenberger, D., Oppliger, W., Dolfini, L., Junne, T., Schatz, G., and Or, E. (2000) Tim18p, a new subunit of the TIM22 complex that mediates insertion of imported proteins into the yeast mitochondrial inner membrane. *Mol. Cell. Biol.* **20,** 1187–1193
22. Gebert, N., Gebert, M., Oeljeklaus, S., von der Malsburg, K., Stroud, D. A., Kulawiak, B., Wirth, C., Zahedi, R. P., Dolezal, P., Wiese, S., Simon, O., Schulze-Specking, A., Truscott, K. N., Sickmann, A., Rehling, P., Guiard, B., Hunte, C., Warscheid, B., van der Laan, M., Pfanner, N., and Wiedemann, N. (2011) Dual function of Sdh3 in the respiratory chain and TIM22 protein translocase of the mitochondrial inner membrane. *Mol. Cell* **44,** 811–818
23. Szeto, S. S., Reinke, S. N., Sykes, B. D., and Lemire, B. D. (2007) Ubiquinone-binding site mutations in the *Saccharomyces cerevisiae* succinate dehydrogenase generate superoxide and lead to the accumulation of succinate. *J. Biol. Chem.* **282,** 27518–27526
24. Oyedotun, K. S., and Lemire, B. D. (1997) The carboxyl terminus of the *Saccharomyces cerevisiae* succinate dehydrogenase membrane subunit, SDH4p, is necessary for ubiquinone reduction and enzyme stability. *J. Biol. Chem.* **272,** 31382–31388
25. Gietz, R. D., and Sugino, A. (1988) New yeast-*Escherichia coli* shuttle vectors constructed with *in vitro* mutagenized yeast genes lacking six-base pair restriction sites. *Gene* **74,** 527–534
26. Oyedotun, K. S., and Lemire, B. D. (1999) The *Saccharomyces cerevisiae* succinate-ubiquinone oxidoreductase. Identification of Sdh3p amino acid residues involved in ubiquinone binding. *J. Biol. Chem.* **274,** 23956–23962
27. Oyedotun, K. S., and Lemire, B. D. (2001) The quinone-binding sites of the *Saccharomyces cerevisiae* succinate-ubiquinone oxidoreductase. *J. Biol. Chem.* **276,** 16936–16943
28. Robinson, K. M., and Lemire, B. D. (1995) Flavinylation of succinate: ubiquinone oxidoreductase from *Saccharomyces cerevisiae*. *Methods Enzymol.* **260,** 34–51
29. Szeto, S. S., Reinke, S. N., Sykes, B. D., and Lemire, B. D. (2010) Mutations in the *Saccharomyces cerevisiae* succinate dehydrogenase result in distinct metabolic phenotypes revealed through ^{1}H NMR-based metabolic footprinting. *J. Proteome Res.* **9,** 6729–6739
30. Reinke, S. N., Hu, X., Sykes, B. D., and Lemire, B. D. (2010) *Caenorhabditis elegans* diet significantly affects metabolic profile, mitochondrial DNA levels, lifespan and brood size. *Mol. Genet. Metab.* **100,** 274–282
31. Eriksson, L., Andersson, P. L., Johansson, E., and Tysklind, M. (2006) Megavariate analysis of environmental QSAR data. Part I—a basic framework founded on principal component analysis (PCA), partial least squares (PLS), and statistical molecular design (SMD). *Mol. Divers.* **10,** 169–186
32. Claros, M. G., and von Heijne, G. (1994) TopPred II: an improved software for membrane protein structure predictions. *Comput. Appl. Biosci.* **10,** 685–686
33. Claros, M. G., and Vincens, P. (1996) Computational method to predict mitochondrially imported proteins and their targeting sequences. *Eur. J. Biochem.* **241,** 779–786
34. Fisher, N., and Rich, P. R. (2000) A motif for quinone binding sites in respiratory and photosynthetic systems. *J. Mol. Biol.* **296,** 1153–1162
35. Rich, P., and Fisher, N. (1999) Generic features of quinone-binding sites. *Biochem. Soc. Trans.* **27,** 561–565
36. Oyedotun, K. S., Yau, P. F., and Lemire, B. D. (2004) Identification of the heme axial ligands in the cytochrome b_{562} of the *Saccharomyces cerevisiae* succinate dehydrogenase. *J. Biol. Chem.* **279,** 9432–9439
37. Guo, J., and Lemire, B. D. (2003) The ubiquinone-binding site of the *Saccharomyces cerevisiae* succinate-ubiquinone oxidoreductase is a source of superoxide. *J. Biol. Chem.* **278,** 47629–47635
38. Ishii, N., Fujii, M., Hartman, P. S., Tsuda, M., Yasuda, K., Senoo-Matsuda, N., Yanase, S., Ayusawa, D., and Suzuki, K. (1998) A mutation in succinate dehydrogenase cytochrome *b* causes oxidative stress and ageing in nematodes. *Nature* **394,** 694–697
39. Oyedotun, K. S., and Lemire, B. D. (2004) The quaternary structure of the *Saccharomyces cerevisiae* succinate dehydrogenase. Homology modeling, cofactor docking, and molecular dynamics simulation studies. *J. Biol. Chem.* **279,** 9424–9431
40. Oyedotun, K. S., Sit, C. S., and Lemire, B. D. (2007) The *Saccharomyces cerevisiae* succinate dehydrogenase does not require heme for ubiquinone reduction. *Biochim. Biophys. Acta* **1767,** 1436–1445
41. Bullis, B. L., and Lemire, B. D. (1994) Isolation and characterization of the *Saccharomyces cerevisiae* SDH4 gene encoding a membrane anchor subunit of succinate dehydrogenase. *J. Biol. Chem.* **269,** 6543–6549
42. Robinson, K. M., von Kieckebusch-Gück, A., and Lemire, B. D. (1991) Isolation and characterization of a *Saccharomyces cerevisiae* mutant disrupted for the succinate dehydrogenase flavoprotein subunit. *J. Biol. Chem.* **266,** 21347–21350
43. Silkin, Y., Oyedotun, K. S., and Lemire, B. D. (2007) The role of Sdh4p Tyr-89 in ubiquinone reduction by the *Saccharomyces cerevisiae* succinate dehydrogenase. *Biochim. Biophys. Acta* **1767,** 143–150
44. Scheffler, I. E. (2001) A century of mitochondrial research: achievements and perspectives. *Mitochondrion* **1,** 3–31
45. Castrillo, J. I., Zeef, L. A., Hoyle, D. C., Zhang, N., Hayes, A., Gardner, D. C., Cornell, M. J., Petty, J., Hakes, L., Wardleworth, L., Rash, B., Brown, M., Dunn, W. B., Broadhurst, D., O'Donoghue, K., Hester, S. S., Dunkley, T. P., Hart, S. R., Swainston, N., Li, P., Gaskell, S. J., Paton, N. W., Lilley, K. S., Kell, D. B., and Oliver, S. G. (2007) Growth control of the eukaryote cell: a systems biology study in yeast. *J. Biol.* **6,** 4
46. Cecchini, G. (2003) Function and structure of complex II of the respiratory chain. *Annu. Rev. Biochem.* **72,** 77–109
47. Tran, Q. M., Rothery, R. A., Maklashina, E., Cecchini, G., and Weiner, J. H. (2007) *Escherichia coli* succinate dehydrogenase variant lacking the heme b. *Proc. Natl. Acad. Sci. U.S.A.* **104,** 18007–18012
48. Kellis, M., Birren, B. W., and Lander, E. S. (2004) Proof and evolutionary analysis of ancient genome duplication in the yeast *Saccharomyces cerevisiae*. *Nature* **428,** 617–624
49. Brasseur, G., Tron, G., Dujardin, G., Slonimski, P. P., and Brivet-Chevillotte, P. (1997) The nuclear ABC1 gene is essential for the correct conformation and functioning of the cytochrome bc_1 complex and the neighbouring complexes II and IV in the mitochondrial respiratory chain. *Eur. J. Biochem.* **246,** 103–111
50. Bruel, C., di Rago, J. P., Slonimski, P. P., and Lemesle-Meunier, D. (1995) Role of the evolutionarily conserved cytochrome *b* tryptophan 142 in the ubiquinol oxidation catalyzed by the bc_1 complex in the yeast *Saccharomyces cerevisiae*. *J. Biol. Chem.* **270,** 22321–22328
51. Oyedotun, K. S., and Lemire, B. D. (1999) The *Saccharomyces cerevisiae* succinate-ubiquinone reductase contains a stoichiometric amount of cytochrome b_{562}. *FEBS Lett.* **442,** 203–207

52. Maklashina, E., Rajagukguk, S., McIntire, W. S., and Cecchini, G. (2010) Mutation of the heme axial ligand of *Escherichia coli* succinate-quinone reductase: implications for heme ligation in mitochondrial complex II from yeast. *Biochim. Biophys. Acta* **1797,** 747–754
53. Horsefield, R., Yankovskaya, V., Sexton, G., Whittingham, W., Shiomi, K., Omura, S., Byrne, B., Cecchini, G., and Iwata, S. (2006) Structural and computational analysis of the quinone-binding site of complex II (succinate-ubiquinone oxidoreductase): a mechanism of electron transfer and proton conduction during ubiquinone reduction. *J. Biol. Chem.* **281,** 7309–7316
54. Miyadera, H., Shiomi, K., Ui, H., Yamaguchi, Y., Masuma, R., Tomoda, H., Miyoshi, H., Osanai, A., Kita, K., and Omura, S. (2003) Atpenins, potent and specific inhibitors of mitochondrial complex II (succinate-ubiquinone oxidoreductase). *Proc. Natl. Acad. Sci. U.S.A.* **100,** 473–477
55. Tran, Q. M., Rothery, R. A., Maklashina, E., Cecchini, G., and Weiner, J. H. (2006) The quinone binding site in *Escherichia coli* succinate dehydrogenase is required for electron transfer to the heme b. *J. Biol. Chem.* **281,** 32310–32317
56. Morales, J., Mogi, T., Mineki, S., Takashima, E., Mineki, R., Hirawake, H., Sakamoto, K., Omura, S., and Kita, K. (2009) Novel mitochondrial complex II isolated from *Trypanosoma cruzi* is composed of 12 peptides including a heterodimeric Ip subunit. *J. Biol. Chem.* **284,** 7255–7263
57. Travers, K. J., Patil, C. K., Wodicka, L., Lockhart, D. J., Weissman, J. S., and Walter, P. (2000) Functional and genomic analyses reveal an essential coordination between the unfolded protein response and ER-associated degradation. *Cell* **101,** 249–258
58. Wyrick, J. J., Holstege, F. C., Jennings, E. G., Causton, H. C., Shore, D., Grunstein, M., Lander, E. S., and Young, R. A. (1999) Chromosomal landscape of nucleosome-dependent gene expression and silencing in yeast. *Nature* **402,** 418–421
59. Smith, J. J., Marelli, M., Christmas, R. H., Vizeacoumar, F. J., Dilworth, D. J., Ideker, T., Galitski, T., Dimitrov, K., Rachubinski, R. A., and Aitchison, J. D. (2002) Transcriptome profiling to identify genes involved in peroxisome assembly and function. *J. Cell Biol.* **158,** 259–271
60. Lai, L. C., Kosorukoff, A. L., Burke, P. V., and Kwast, K. E. (2006) Metabolic-state-dependent remodeling of the transcriptome in response to anoxia and subsequent reoxygenation in *Saccharomyces cerevisiae*. *Eukaryot. Cell* **5,** 1468–1489
61. Chu, S., DeRisi, J., Eisen, M., Mulholland, J., Botstein, D., Brown, P. O., and Herskowitz, I. (1998) The transcriptional program of sporulation in budding yeast. *Science* **282,** 699–705
62. Roberts, G. G., and Hudson, A. P. (2006) Transcriptome profiling of *Saccharomyces cerevisiae* during a transition from fermentative to glycerol-based respiratory growth reveals extensive metabolic and structural remodeling. *Mol. Genet. Genomics* **276,** 170–186
63. Gasch, A. P., Spellman, P. T., Kao, C. M., Carmel-Harel, O., Eisen, M. B., Storz, G., Botstein, D., and Brown, P. O. (2000) Genomic expression programs in the response of yeast cells to environmental changes. *Mol. Biol. Cell* **11,** 4241–4257
64. Ferea, T. L., Botstein, D., Brown, P. O., and Rosenzweig, R. F. (1999) Systematic changes in gene expression patterns following adaptive evolution in yeast. *Proc. Natl. Acad. Sci. U.S.A.* **96,** 9721–9726
65. Sickmann, A., Reinders, J., Wagner, Y., Joppich, C., Zahedi, R., Meyer, H. E., Schönfisch, B., Perschil, I., Chacinska, A., Guiard, B., Rehling, P., Pfanner, N., and Meisinger, C. (2003) The proteome of *Saccharomyces cerevisiae* mitochondria. *Proc. Natl. Acad. Sci. U.S.A.* **100,** 13207–13212
66. Krogan, N. J., Cagney, G., Yu, H., Zhong, G., Guo, X., Ignatchenko, A., Li, J., Pu, S., Datta, N., Tikuisis, A. P., Punna, T., Peregrín-Alvarez, J. M., Shales, M., Zhang, X., Davey, M., Robinson, M. D., Paccanaro, A., Bray, J. E., Sheung, A., Beattie, B., Richards, D. P., Canadien, V., Lalev, A., Mena, F., Wong, P., Starostine, A., Canete, M. M., Vlasblom, J., Wu, S., Orsi, C., Collins, S. R., Chandran, S., Haw, R., Rilstone, J. J., Gandi, K., Thompson, N. J., Musso, G., St Onge, P., Ghanny, S., Lam, M. H., Butland, G., Altaf-Ul, A. M., Kanaya, S., Shilatifard, A., O'Shea, E., Weissman, J. S., Ingles, C. J., Hughes, T. R., Parkinson, J., Gerstein, M., Wodak, S. J., Emili, A., and Greenblatt, J. F. (2006) Global landscape of protein complexes in the yeast *Saccharomyces cerevisiae*. *Nature* **440,** 637–643
67. Ebeler, S. E. (2001) Analytical chemistry: Unlocking the secrets of wine flavor. *Food Rev. Int.* **17,** 45–64
68. Arikawa, Y., Kobayashi, M., Kodaira, R., Shimosaka, M., Muratsubaki, H., Enomoto, K., and Okazaki, M. (1999) Isolation of sake yeast strains possessing various levels of succinate- and/or malate-producing abilities by gene disruption or mutation. *J. Biosci. Bioeng.* **87,** 333–339
69. Polychroniadou, E., Kanellaki, M., Iconomopoulou, M., Koutinas, A. A., Marchant, R., and Banat, I. M. (2003) Grape and apple wines volatile fermentation products and possible relation to spoilage. *Bioresour. Technol.* **87,** 337–339
70. Romano, P., Fiore, C., Paraggio, M., Caruso, M., and Capece, A. (2003) Function of yeast species and strains in wine flavour. *Int. J. Food Microbiol.* **86,** 169–180
71. Thompson, J. D., Gibson, T. J., and Higgins, D. G. (2002) Multiple sequence alignment using ClustalW and ClustalX. *Curr. Protoc. Bioinformatics* Chapter 2, Unit 2.3
72. Daignan-Fornier, B., Valens, M., Lemire, B. D., and Bolotin-Fukuhara, M. (1994) Structure and regulation of SDH3, the yeast gene encoding the cytochrome b_{560} subunit of respiratory complex II. *J. Biol. Chem.* **269,** 15469–15472